JTTEE5 5:277-282

Effects of High-Pressure Plasma Spraying for Yttria-Stabilized Zirconia Coating

S. Sodeoka, M. Suzuki, and K. Ueno

Plasma spraying of yttria-stabilized zirconia was carried out under chamber pressures ranging from low (30 kPa) to high pressure (300 kPa) to investigate pressure effects on the plasma jet and to clarify the potential of high-pressure plasma spraying (HPPS) as a high performance coating tool. Plasma flame length and velocity of the particles were measured in situ, and the coating characteristics including its microstructure, density, and hardness were studied. A condensed plasma flame under high pressure facilitated sufficient melting of zirconia particles, resulting in high deposition efficiency and a dense coating with improved hardness, in spite of reduced particle velocity. High-pressure plasma spraying was found to be suitable for thermal spraying of high-melting-point materials such as zirconia.

Keywords arc characteristics, high-pressure plasma spraying, material properties, zirconia feedstock

1. Introduction

THE ATMOSPHERE surrounding the plasma torch strongly affects the properties of the plasma flame. In cases of low pressures (less than 10 kPa), the plasma jet extends and an extremely high velocity stream can be obtained (Ref 1-3). Such plasma jets are used to prepare dense metal coatings such as bond coatings for thermal barrier applications. This process is known as low-pressure plasma spraying (LPPS). However, when LPPS is applied to high-melting-point materials such as ceramics, it often suffers from poor heating capacity because of the decrease of the energy density of the plasma due to the flame extension and the low heat transfer from plasma to feedstock. As a result, the deposition efficiency decreases compared with that of ordinary atmospheric plasma spraying (APS).

On the other hand, it can be expected that the plasma generated in a high-pressure chamber may have improved heating ability. Jager et al. (Ref 4) have reported the effectiveness of high-pressure plasma spraying (HPPS) pressures up to 200 kPa (2 atm). They concluded that B_4C showed improved spray efficiencies and a better degree of melting with rising pressure; however, little information about the pressure effect on the properties of the coating was described. In this work, the authors

S. Sodeoka, M. Suzuki, and **K. Ueno,** Osaka National Research Institute, Agency of Industrial Science and Technology, Midorigaoka 1-8-31, Ikeda 563 Osaka, Japan.

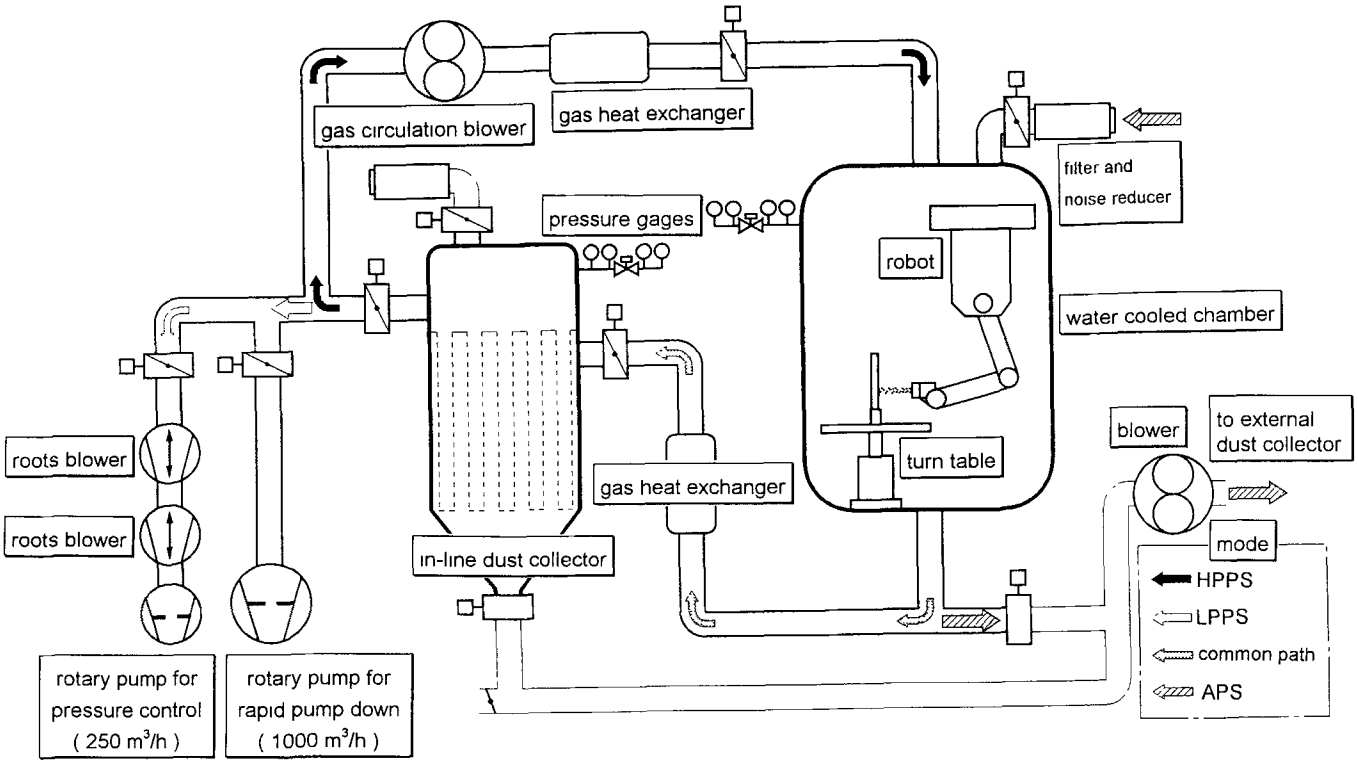

Fig. 1 CAPS system

studied the plasma jet under pressures up to 300 kPa and performed spraying experiments with yttria-stabilized zirconia. The velocity of the in-flight particles was determined, and the properties of the deposit were evaluated.

2. Experimental

2.1 *Spraying Equipment*

Figure 1 illustrates the schematic outline of the HPPS system used in this work. It is termed a CAPS (controlled-atmosphere plasma spraying) system and is manufactured by Plasma-Technik (Wohlen, Switzerland). This system was designed for plasma spraying in the 1 to 500 kPa pressure range, which covers many types of plasma spraying, including LPPS, APS, and HPPS in inert gas. Reactive plasma spraying in gas such as nitrogen is also possible. During HPPS, the chamber gas circulates through the cooling path, in which two heat exchangers and a dust remover are incorporated, and returns to the spraying chamber for gas recycling. Either the EPI-03CP 120 kW gun (Electro-Plasma, Inc., Millbury, OH) or PT F4VB 55 kW gun (Plasma-Technik, Wohlen, Switzerland) is available for this system, and in this work the EPI gun with a specially designed high-cooling-efficient nozzle enabled an input power up to 120 kW.

2.2 *Spraying Conditions*

Thermal spraying was carried out under chamber pressures of 30, 115, 200, and 300 kPa (Table 1). As a spray material, spray-dried 8 wt% yttria-stabilized zirconia powder, YSZ (AMDRY 6610, Sulzer Plasma Technik, Inc., Troy, MI) was used. Carbon steel substrates (JIS SS400, size: 100 by 100 by 3 mm) were blasted with alumina grit (No. 70, Japan Abrasive Co. Ltd., Sakai, Japan) just before spraying. The chamber was pumped out to a pressure of 1 Pa, and then argon gas was backfilled to a prescribed pressure.

2.3 *Evaluation Methods*

The plasma flame was observed with a standard video camera through a window in the chamber, and the flame length was measured on the still picture. The velocity of the in-flight particle was estimated from the length of glowing traces on the photographs recorded by a high-speed-camera (ULTRANAC FS501, Imco Electro-Optics Ltd., Basilden, UK) with an exposure period of 20 μs.

Deposition efficiency was defined as a ratio of the weight gain to the amount of fed powder within a certain spray time.

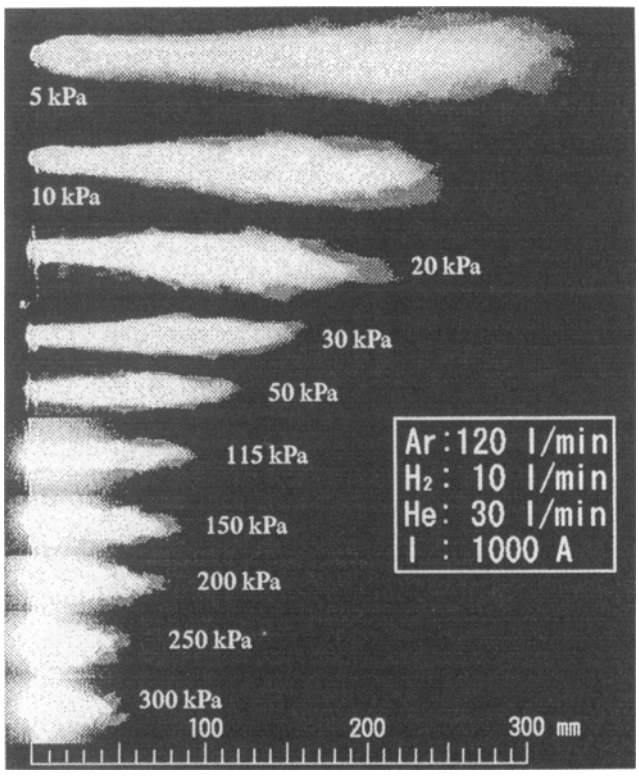

Fig. 2 Typical images of plasma flame under various chamber pressures

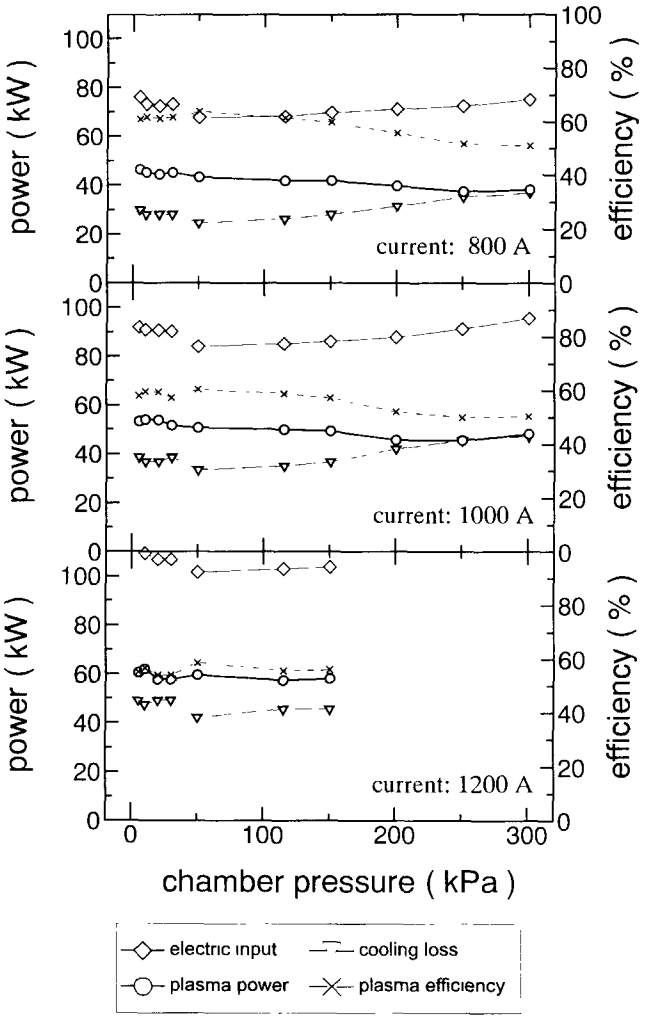

Fig. 3 Dependence of power balance on chamber pressure and electric current with constant plasma gas flow (2.0×10^{-3} m^3/s Ar, 1.7×10^{-4} m^3/s H_2 5.0×10^{-4} m^3/s He)

The free-standing deposit was separated from the substrate by etching in hydrochloric acid, and its bulk density was measured by the water-immersion method.

Crystallographic phases were determined by the x-ray diffraction (XRD) technique. The coating microstructure was examined by scanning electron microscopy (SEM). Vickers microhardness (with at least 15 tests performed) was measured on the polished cross section of the deposit at an indentation load of 2.94 N for 15 s.

Table 1 Plasma spraying parameters for HPPS of yttria-stabilized zirconia coating

System	Plasma-Technik CAPS system
Gun (nozzle, cathode)	EPI-03CP (03CPP-102, 03CA-27)
Chamber pressure, kPa	
For spraying	30, 115, 200, 300
To characterize plasma	5-300
Spraying distance, mm	250, 200, 140, 120
Plasma gas flow rate, L/min	
Ar	120
H_2	5
He	30
Electric current, A	
For spraying	800
To characterize plasma	800, 1000, 1200
Electric voltage, V	90.7-99.0
Powder	AMDRY 6610
Powder feed rate, g/min	25
Powder carrier gas, L/min, Ar	5.0-6.5
Substrate cooling	No cooling

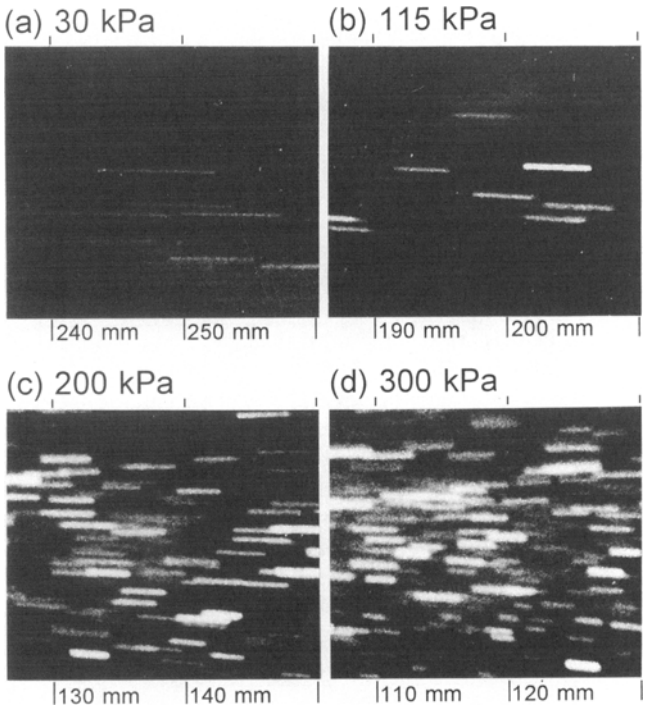

Fig. 4 Trace of flying particles during 20 μs. (a) Chamber pressure, 30 kPa; distance from nozzle outlet, ≈250 mm. (b) 115 kPa, 200 mm. (c) 200 kPa, 140 mm (d) 300 kPa, 120 mm

3. Results and Discussion

3.1 *Plasma Flame Observation*

The effect of chamber pressure on plasma characteristics was evaluated by observing the flame under pressures from 5 to 300 kPa (Fig. 2). The flame length under 5 kPa extended to about 300 mm, but decreased as chamber pressure was raised. Under a pressure of 300 kPa, the flame length was about 50 mm, showing that the high-temperature zone was condensed. The high flame brightness indicated that the volume density of plasma energy increased in such a condensed flame. This was also confirmed by the color of the flame edge, which changed from red-purple under low pressure to glowing white under high pressure.

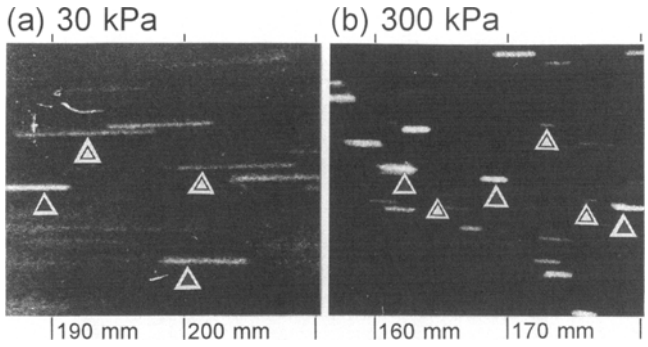

Fig. 5 Differences in particle traces with respect to particle size. (a) 30 kPa. (b) 300 kPa

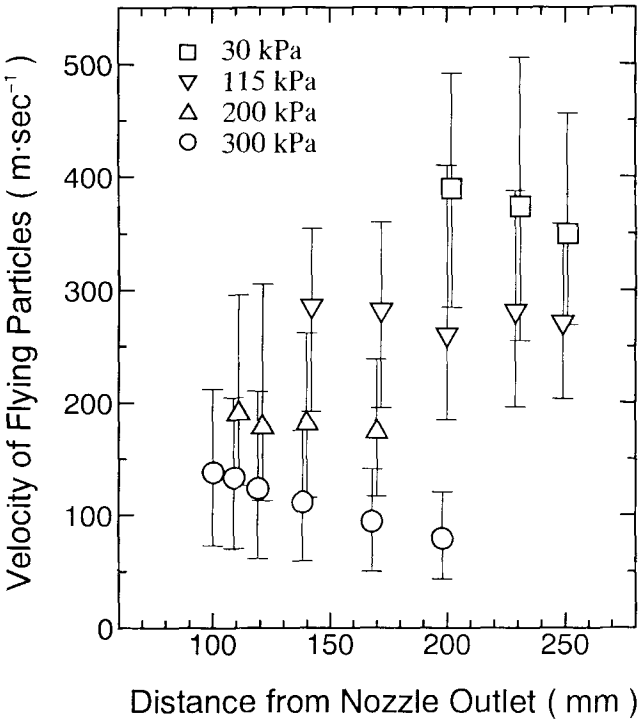

Fig. 6 Relationship among chamber pressure, distance from nozzle outlet, and particle velocity determined by measuring trace length on high-speed-photographs

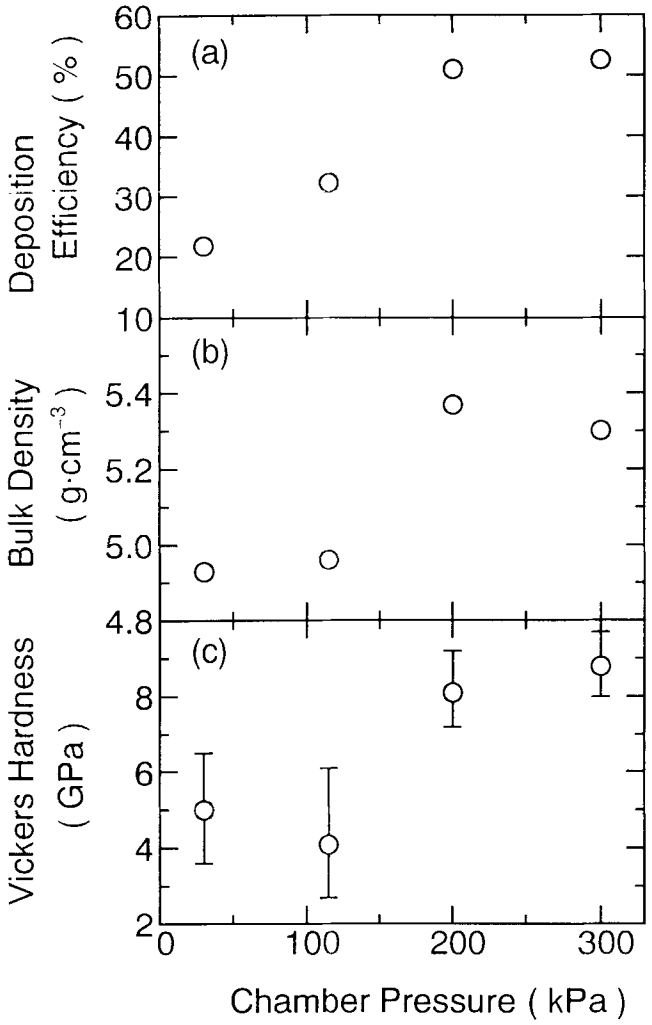

Fig. 7 Change in deposition efficiency, bulk density, and Vickers microhardness with chamber pressure

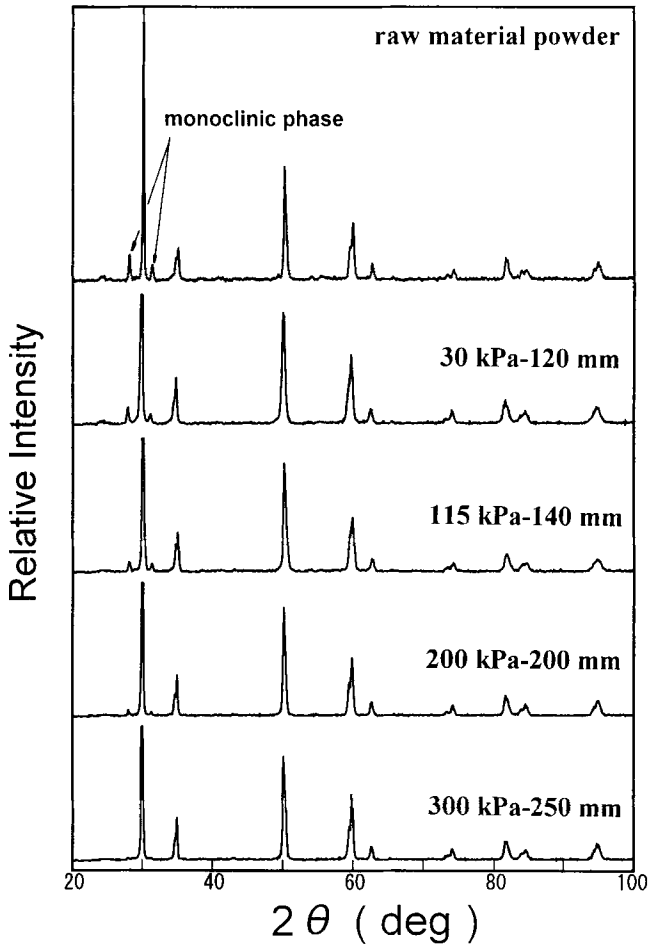

Fig. 8 XRD patterns of raw material powder and deposits sprayed in various chamber pressure, measured with Cu-Kα

3.2 *Power Balance*

It is important to know the efficiency of energy conversion from electric power to plasma energy under high pressure. A shrunken plasma flame under high pressure is expected to allow better heating of injected spray powder, but at the same time, it also encloses the heat within the nozzle. As a result, the nozzle is severely heated and heat loss through the nozzle wall to the cooling water increases with increasing chamber pressure. The temperature difference between inlet and outlet water for gun cooling and its flow rate allows calculation of the cooling loss through the nozzle wall (Ref 4). Plasma power, which was used to generate the plasma, was defined as the difference between the input electric power and the cooling loss. Plasma efficiency was defined as the ratio of plasma power to input electric power and indicated the quantity of input energy converted to the plasma energy. Figure 3 shows the chamber-pressure dependence of electric power, plasma power, cooling loss, and plasma efficiency when the electric current is 800, 1000, and 1200 A, respectively. Electric input power increased as the chamber pressure exceeded ambient pressure (115 kPa) due to the fact that the discharging voltage increased with increasing pressure. At the same time, the cooling loss also increased because of the plasma shrinkage, as described above. Therefore, the input electric power increased with increasing pressure, but the plasma power did not increase; in fact, it decreased slightly. Thus the efficiency for converting electric power to plasma energy significantly decreased with increasing chamber pressure, as shown in Fig. 3 (top) and (middle). The increase of current raised both of electric power and plasma power, but also further increased cooling loss, resulting in a decrease of plasma efficiency.

The technical difficulty is that the cooling capacity of the water running through the nozzle has a certain limitation, and if the power exceeds this limit then there is high possibility of nozzle melt down. As shown in Fig. 3 (bottom), the maximum pressure achieved without nozzle damage at 1200 A was 150 kPa. To suppress this overheating of the gun, a high-plasma gas flow and addition of helium gas with high heat conductivity was used to select stable and safety spraying conditions within the restricted range. Improvements in nozzle design for HPPS are needed.

3.3 *Velocity of Flying Particles*

Figure 4 shows typical photographs of in-flight particles exiting the flame. The photographs were taken with a high-speed-

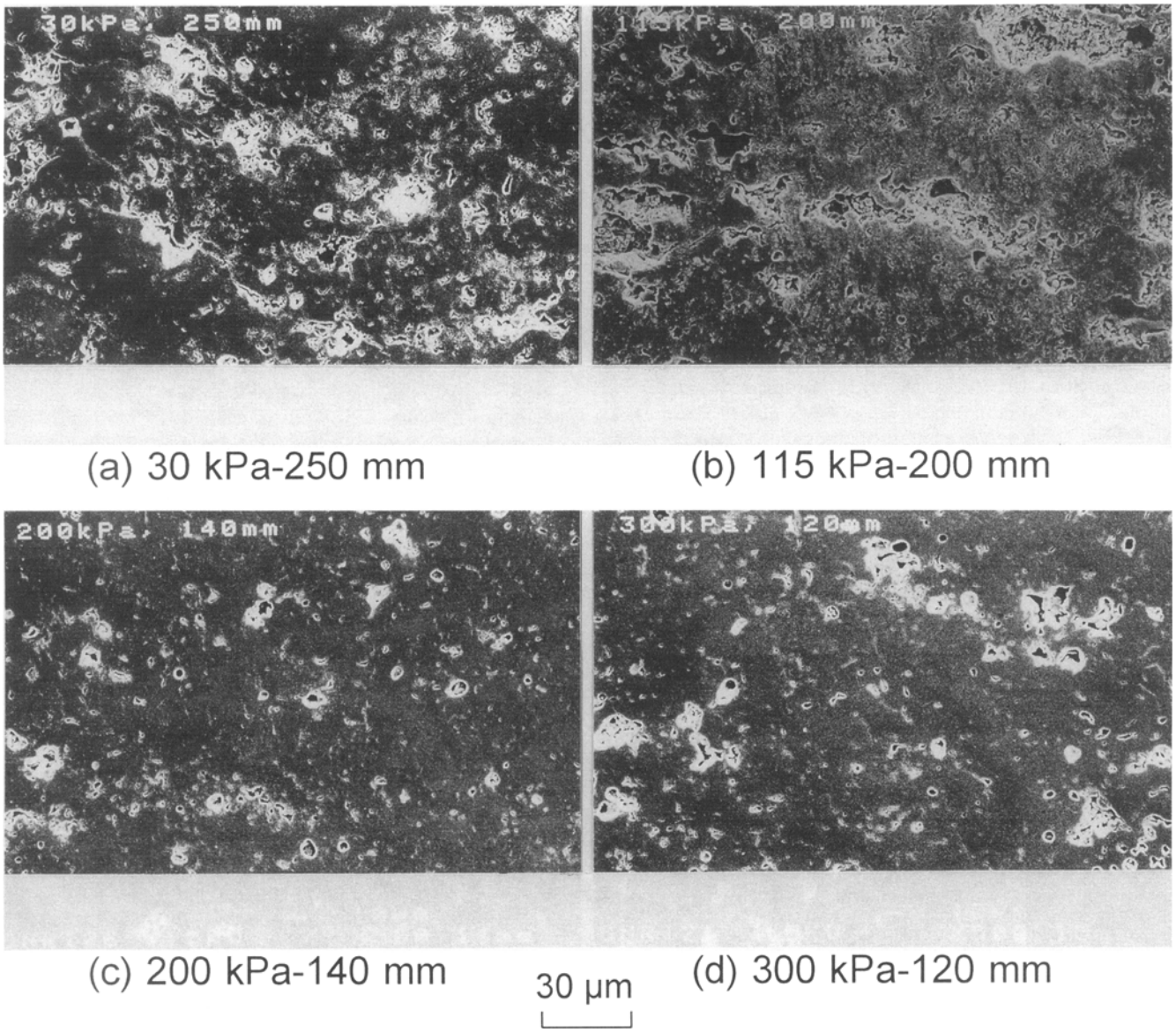

Fig. 9 Scanning electron micrographs of polished cross section of yttria-stabilized zirconia deposits sprayed in various chamber pressure and spraying distance. (a) 30 kPa, 250 mm. (b) 115 kPa, 200 mm. (c) 200 kPa, 140 mm. (d) 300 kPa, 120 mm

camera at an exposure time of 20 μs. The length, brightness, and width of these white lines reflect velocity, temperature, and size of each flying particle, respectively. The scale below each photo indicates the distance from the nozzle outlet. These photos show that the higher the chamber pressure, the shorter the line length, and therefore, the slower the particle velocity. Similar phenomena have been reported for LPPS (Ref 3). The number of bright lines (i.e., well-heated particles) significantly increased with increasing chamber pressure, confirming that high-pressure spraying is effective for heating feedstock.

It has also been observed that the smaller particle (thin line, Δ) is considerably faster than the larger one (thick line, ▲) under low pressure as indicated in Fig. 5(a). In contrast with this, the smaller one (Δ) is rather slower than the larger one (▲) under high pressure (Fig. 5b). This effect probably arises from aerodynamic drag.

The relationship among the particle velocity, chamber pressure, and the distance from the nozzle outlet is shown in Fig. 6. The particle velocity decreases with increasing chamber pressure, and a kinetic effect cannot be expected when the molten sprayed particle impinges on a substrate under high pressure, unlike HVOF spraying.

On the other hand, as the distance from the nozzle outlet increases, the velocity of particles decreases, but the degree of speed reduction is relatively smaller in the medium-pressure range from 115 to 200 kPa. These values are much higher than typical spraying parameters (Ref 5) because high plasma gas flow as described in the section 3.1 has been selected.

3.4 *Coating Properties*

Figure 7 shows the chamber pressure dependency of deposition efficiency, bulk density and Vickers hardness. The spray distances were 250 mm at 30 kPa, 200 mm at 115 kPa, 140 mm at 200 kPa, and 120 mm at 300 kPa. Deposition efficiency (Fig. 7, top) increased with increasing chamber pressure up to 200 kPa, but the increase saturated at about 52% over this pressure. It seemed that the flame at 200 kPa had sufficient heating capacity for melting zirconia powder. Optimization of other parameters such as powder inlet position is necessary to further improve the deposition efficiency.

Bulk density (Fig. 7, middle) increased distinctively when the pressure exceeded 200 kPa, but the density of the coating sprayed at 300 kPa was lower than that at 200 kPa. This probably arises from the low-particle velocity as described in the previous section. The maximum relative density was 92% when sprayed at 200 kPa. The hardness (Fig. 7, bottom) shows a similar pressure dependence as the bulk density. The maximum value was 8.8 GPa for the coating sprayed at 300 kPa, two times higher than the coatings sprayed under ambient or low pressure. The hardness value for HPPS coatings reached two-thirds of the hardness of sintered yttria-stabilized zirconia (Ref 5, 7). Therefore, under high pressure the zirconia particles were melted sufficiently that lamella combined strongly with each other. The coating fabricated at 50 kPa exhibits a higher hardness than that fabricated at 115 kPa and this could arise from the high velocities experienced in LPPS.

It was concluded that the high-pressure spraying was significantly effective in heating the feedstock and fabricating dense coatings with higher hardness. In addition, improved heating also brings about high deposition efficiency.

3.5 *Crystallographic Phase and Microstructure*

All deposits were gray, although the color of the feedstock powder was cream-yellow. This is probably due to oxygen loss from the zirconia lattice during the spraying. The color of deposits becomes darker as the chamber pressure increases. Detailed examination of the profiles revealed that the fraction of monoclinic phase decreased with increasing chamber pressure (Fig. 8). This could be explained by considering the cooling rate of molten particles. Thus, although there is no data concerning the substrate temperature during spraying, it is feasible that the heat transfer from the molten particle to the surrounding gas increases with increasing pressure. Thus, the molten particle sprayed under high pressure was cooled more rapidly than under low pressure. Therefore, a large amount of high-temperature phase (tetragonal) was retained through quenching on deposition under high pressure (Ref 8). This is in agreement with the chamber pressure dependence of the coating characteristics as described above.

Figures 9 (a) to (d) show the polished cross sections of the deposits sprayed under 30, 115, 200, and 300 kPa, respectively. The coarse pores disappeared as the chamber pressure increased, corresponding with the bulk density as shown in Fig. 7. When the chamber pressure is high (Fig. 9c and d), it is difficult to distinguish lamella boundaries, suggesting that the sprayed particles are sufficiently molten under high pressure to form good interlamellar contact. These results also confirm the improved heating capability of HPPS.

4. Conclusions

The effect of the chamber pressure on plasma flame, sprayed particle velocity, and the coating characteristics was investigated. When the chamber pressure increased, the plasma flame shortened and the brightness of the flame increased. Although the velocity of the powder decreased under high pressures, the heating efficiency increased on account of the concentrated thermal energy within the shrunken flame. It was found that the HPPS is very effective in improving the deposition efficiency and the hardness of the coating in the thermal spraying of high-melting-point materials such as zirconia. In order to apply HPPS to the industrial field, however, it is necessary to study further the properties of the plasma under high pressure and improve the devices and the operating system for obtaining stable plasma plumes and selecting wider spraying conditions under high pressure.

References

1. D. Apelian, D. Wei, and M. Paliwal, Particle-Plasma Interactions during Low Pressure Plasma Deposition, *Thin Solid Films,* Vol 118, 1984, p 395-407
2. S. Amade, T. Senda, S. Uematu, and C. Iino, Heating Process of a Ceramic Particle by Plasma Flow under Reduced Pressure, *J. Jpn. Therm. Spray. Soc.*, Vol 27 (No. 4), 1990, p 220-227 (in Japanese)
3. M.F. Smith and R.C. Dykhuizen, The Effect of Chamber Pressure on Particle Velocities in Low-Pressure Plasma Spray Deposition, *Thermal Spray: Advances in Coatings Technology,* D.L. Houck, Ed., ASM International, 1988, p 21-24
4. D.A. Jager, D. Stover, and W. Schlump, High Pressure Plasma Spraying in Controlled Atmosphere Up to Two Bar, *Thermal Spray: International Advances in Coating Technology,* C.C. Berndt, Ed., ASM International, 1992, p 69-74
5. S. Sodeoka, K. Ueno, and T. Inoue. Structure and Properties of Low-Pressure-Plasma-Sprayed Yttria Stabilized Zirconia Coatings, *J. Jpn. Therm. Spray. Soc.*, Vol 31 (No. 2), 1994, p 72-78 (in Japanese)
6. K.Y. Chia, S.G. Seshadri, and S.M. Kunz, Mechanical Behavior of PSZ at Elevated Temperatures, *Ceram. Eng. Sci.*, Vol 7, 1986, p 784-794
7. M. Inada, T. Maeda, and T. Shikata, HIP of Plasma Spray Coated Ceramics, *Proc. Int. Symp. on Advanced Thermal Spraying Technology and Allied Coatings,* High Temperature Society of Japan, 1988, p 211-215
8. V.S. Stubican and J.R. Hellmann, Phase Equilibria in Some Zirconia Systems, *Advances in Ceramics,* Vol 3, *Science and Technology of Zirconia,* A H. Heuer and L.W. Hobbs, Ed., American Ceramic Society, 1981, p 25-36